Molecular Crystals and Liquid Crystals

ISSN: 1542-1406 (Print) 1563-5287 (Online) Journal homepage: http://www.tandfonline.com/loi/gmcl20

Highly Luminescent Red Phosphorescent OLED with Interfacial Layers for Hole Transport and Electron Injection

Jun Ho Lee, Jae Min Kim & Ji Geun Jang

To cite this article: Jun Ho Lee, Jae Min Kim & Ji Geun Jang (2015) Highly Luminescent Red Phosphorescent OLED with Interfacial Layers for Hole Transport and Electron Injection, Molecular Crystals and Liquid Crystals, 618:1, 13-20, DOI: 10.1080/15421406.2015.1075837

To link to this article: http://dx.doi.org/10.1080/15421406.2015.1075837

Mol. Cryst. Liq. Cryst., Vol. 618: pp. 13–20, 2015

ISSN: 1542-1406 print/1563-5287 online
DOI: 10.1080/15421406.2015.1075837

Highly Luminescent Red Phosphorescent OLED with Interfacial Layers for Hole Transport and Electron Injection

JUN HO LEE, JAE MIN KIM, AND JI GEUN JANG*

Department of Electronics Engineering, Dankook University, Chungnam, Korea

Four kinds of red phosphorescent organic light-emitting devices were fabricated and compared to investigate the effect of interfacial layers for hole transport and electron injection. 1 nm-thick LiF in the device A and C and 1 nm-thick Cs_2CO_3 in the device B and D were deposited as an electron injection layer between the anode and the electron transport layer, and 5 nm-thick layer of dipyrazion[2,3-f:2′,2′-h]quinoxaline-2,3,6,7,10,11-hexacarbonitrile[HATCN] was inserted as a hole transport interfacial layer between the hole injection layer and the hole transport layer only in the device C and D. Under a luminance of 1000 cd/m^2, the power efficiencies were 7.6 lm/W and 8.5 lm/W in the device A and B, and 8.6 lm/W and 13.4 lm/W in the device C and D. The quantum efficiency of the device D was 15.8% under 1000 cd/m^2 which was somewhat lower than those of the device A and C, but a little higher than that of the device B. The luminance of the device D was much higher than those of the other devices at a given votage. The luminance of the device D at 7 V was 23,710 cd/m^2, which was 13.0, 3.4, and 4.0 times higher than those of the device A, B, and C at the same voltage, respectively.

Keywords PhOLED; interfacial layer; HATCN; Cs_2CO_3; luminance; quantum efficiency

1. Introduction

High current flow at low operating voltage in organic light-emitting devices (OLEDs) is a key issue because it is directly related to high luminance and low power consumption. Operating voltage and current density of an organic light-emitting device are greatly affected by electron injection from the cathode and hole transport from the anode into the emissive layer. Various approaches for efficient electron injection and enhanced hole transport have been attempted so far. One of the methods for efficient electron injection is to insert an thin interfacial layer of LiF between the cathode and the electron transport layer (ETL) [1–3]. The insertion of thin LiF layer makes it possible to inject electron easily from the cathode into the ETL due to injection barrier lowering and quantum mechanical tunneling without direct contact of organic material and metal. However, the use of LiF as an electron injection layer (EIL) limits electron injection from the cathode to some extent due to its insulating

*Address correspondence to Ji Geun Jang, Department of Electronics Engineering, Dankook University, San 29, Anseo-dong, Cheonan, Chungnam 330-714, Korea (ROK). E-mail: semicgk@dankook.ac.kr

Color versions of one or more of the figures in the article can be found online at www.tandfonline.com/gmcl.

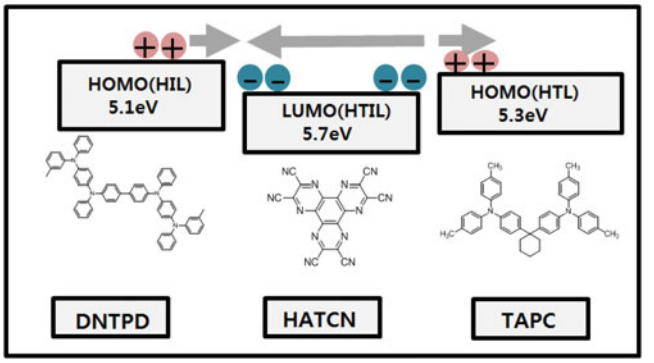

Figure 1. Hole transport by the HATCN in the structure of DNTPD/HATCN/TAPC.

characteristics even though the thickness of LiF is thin enough. For efficient hole injection, a hole injection layer (HIL) can be placed between anode and hole transport layer (HTL) [4–6]. Hole mobility of the HTL should be high to enhance hole transporting property. P-type doping in the HTL can be also adopted to increase hole current density [7,8], but the chemical doping in the organic material involves the process complexity. In this study, luminance and efficiency of red phosphorescent organic light-emitting devices (PhOLEDs) with/without the hole transport interfacial layer (HTIL) of HAT-CN between HIL and HTL utilizing the thin LiF or Cs_2CO_3 layer as an EIL were compared and discussed. Cs_2CO_3 is known to be more effective than LiF as an EIL in OLEDs because it facilitates electron injection from the Al cathode due to the removal of electron barrier height in the EIL [9–11]. The lowest unoccupied molecular orbital (LUMO) and highest occupied molecular orbital (HOMO) energy levels of HATCN were reported to be 5.7 eV and 9.5 eV, respectively [12,13]. The LUMO level of HATCN is deep enough to provide the charge recombination-generation interface between HOMO levels of N,N′-diphenyl-N,N′-bis-[4-(phenyl-m-tolyl-amino)-phenyl]bi-phenyl-4,4′diamine[DNTPD] and 1,1-bis(di-4-tolyamino- phenyl) cyclohexane[TAPC]. DNTPD with a HOMO level of 5.1 eV [14] and TAPC with a HOMO level of 5.3 eV [15] were used as the HIL and the HTL in our devices, respectively. Figure 1 shows the role of HATCN for hole transport in the structure of DNTPD/HATCN/TAPC. The LUMO level of HATCN is closely aligned to the HOMO levels of DNTPD and TAPC as shown in Fig. 1. The electron transfer from the HOMO of TAPC to the LUMO of HATCN and the hole transfer from the HOMO of DNTPD to the LUMO of HATCN can be easily induced due to little energy barrier. The hole injection from the DNTPD to the TAPC can be enhanced by the recombination and generation of electron and hole through the HATCN. When a HATCN layer is interfaced between HIL and HTL, one interface can work as a charge recombination site and the other interface as a a charge generation site. In this case, strong coulombic interaction can exist at the interface between the LUMO of HATCN and the HOMO of DNTPD. The strong coulombic interaction induces the rapid recombination between electrons and holes, which may be the origin of high current density and high luminance.

2. Experimental Methods

The substrates with an ITO anode of 12 Ω/sq on glass were cleaned by chemical process with acetone, methanol, and isopropyl alcohol. The remaining solvent was removed by

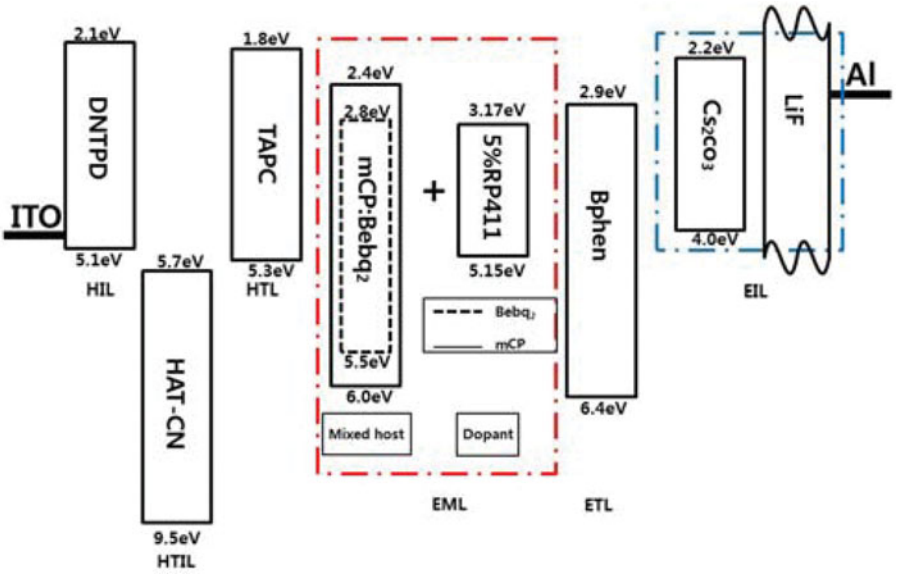

Figure 2. Schematic structure of the fabricated devices and energy level diagram of the used materials.

softbaking for 10 minutes at 100°C. To improve the surface morphology of anode, the plasma treatment was executed at 150 W for two minutes under 8 mTorr of O_2:Ar = 2:1. The plasma treatment before deposition of organic materials reduces the energy barrier for hole injection from anode and removes the surface contaminants [16].

In the deposition of organic/inorganic layers to fabricate the devices, four kinds of methods were used according to the device types (A∼D). Firstly, 50 nm-thick DNTPD was deposited in common as a HIL. And then, 5 nm-thick HATCN was selectively

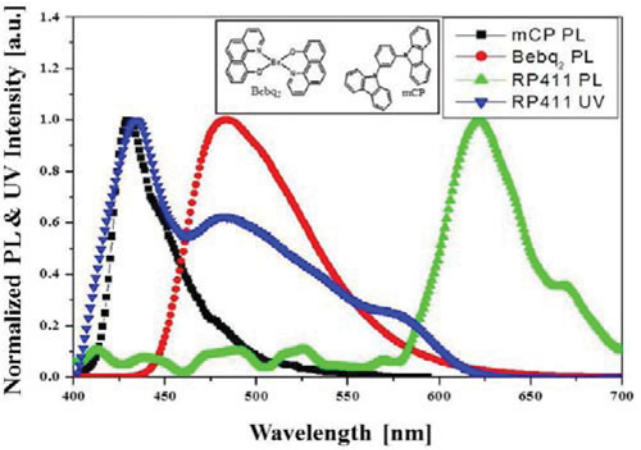

Figure 3. PL spectra of mCP/ $Bebq_2$ and UV-vis absorption/ PL spectra of RP411 with the inset of chemical structures of mCP and $Bebq_2$.

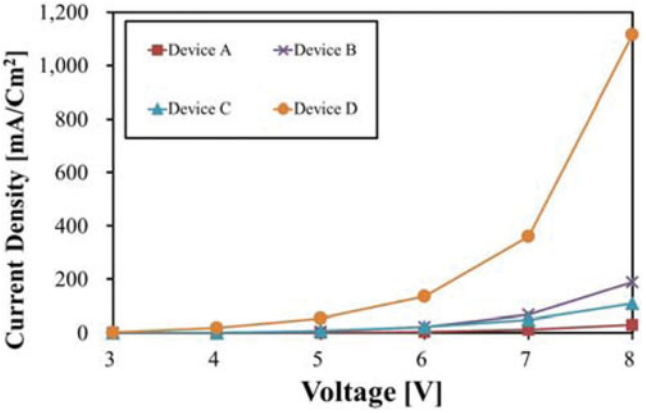

Figure 4. Current density-voltage characteristics of the fabricated devices.

deposited only in the device C and D. Next, 30 nm-thick TAPC was commonly deposited as a HTL. In the formation of emissive layer (EML), the mixed layer of bis(10-hydroxy-benzo[h]quinolinato)beryllium[$Bebq_2$] and N,N′-dicarbazolyl-3,5-benzene[mCP] doped with 5 vol.% RP411 (proprietary red phosphor-rescent dye from SFC Co.) was co-evaporated with thickness of 30 nm as a red emitter. And then, 4,7-diphenyl-1,10-phen anthroline[Bphen] was commonly deposited with thickness of 30 nm as an ETL. As an EIL before the Al cathode, 1 nm-thick LiF layer in the device A and C, and 1 nm- thick in the device B and D were deposited. Finally, 120 nm-thick Al was deposited as the cathode. All organic/inorganic layers in the experiments were deposited by in-situ method under 5×10^{-7} Torr. The structures of four red PhOLEDs named device A, B, C, and D were as follows:

Device A: ITO/DNTPD/TAPC/(mCP,$Bebq_2$):RP411)/Bphen/LiF/Al
Device B: ITO/DNTPD/TAPC/(mCP,$Bebq_2$):RP411)/Bphen/Cs_2CO_3/Al
Device C: ITO/DNTPD/HATCN/TAPC/(mCP,$Bebq_2$):RP411)/Bphen/LiF/Al
Device D: ITO/DNTPD/HATCN/TAPC/(mCP,$Bebq_2$):RP411)/Bphen/Cs_2CO_3/Al

Figure 2 shows the schematic structure of the fabricated devices and the energy level diagram of the used materials. The electroluminescent characteristics such as current density,

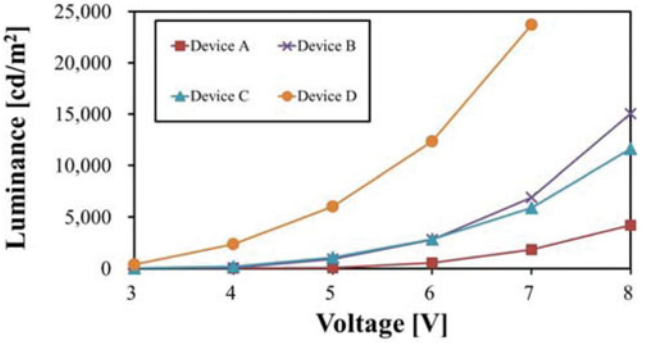

Figure 5. Luminance-voltage characteristics of the fabricated devices.

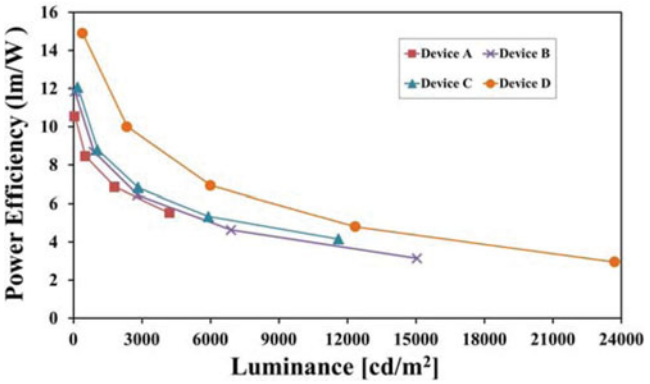

Figure 6. Power efficiency-luminance characteristics of the fabricated devices.

luminance, power and quantum efficiencies, electroluminescence spectra, and Commission Internationale de I'Eclairage (CIE) color coordinates were measured with a Polaronix M6100 test system (McScience) and a CS-1000 spectro-radiometer (Konica Minolta) in a dark condition.

3. Results and Discussion

The DNTPD with a HOMO level of 5.1 eV makes hole injection easy from the ITO anode. The hole mobility and triplet energy of TAPC are known to be 0.01 cm^2/Vs and 2.87 eV[17]. The LUMO barrier of 0.6 eV at the interface of the EML and TAPC is sufficiently large to confine the electrons injected from the cathode into the emitter. Therefore, the TAPC can be used as a good hole transport material in the red PhOLEDs due to high hole mobility and good electron confinement. Moreover, the excitons with triplet energy of 1.98 eV from the phosphor- rescent dye of RP411 can be conserved well through the HTL due to high triplet energy of TAPC. The holes injected from the anode into the emitter can be confined well by the ETL due to high HOMO barrier of 0.4 eV at the interface of the EML and Bphen. The triplet energy of Bphen is also higher than that of RP411 so that the excitons

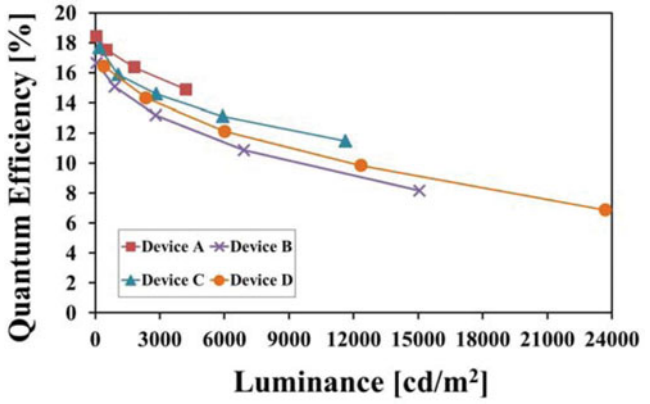

Figure 7. Quantum efficiency- luminance characteristics of the fabricated devices.

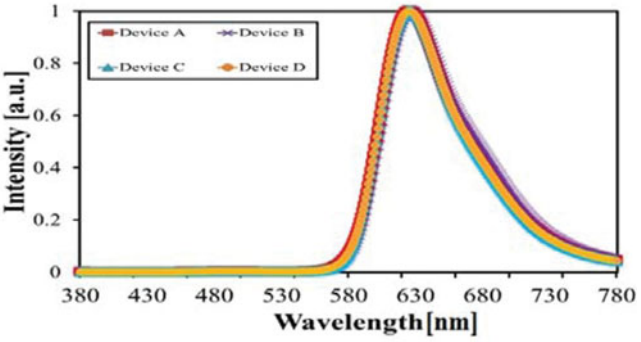

Figure 8. EL spectra of the fabricated devices under an applied voltage of 7V.

can be also protected well in this region. The use of $Bebq_2$ as a co-host with mCP in the EML enhances electron injection from the ETL into the EML and electron transport in the EML due to the lowering of LUMO barrier at the interface of the EML and Bphen and the relative high electron mobility of $Bebq_2$. Figure 3 shows the photoluminescence (PL) spectra of mCP/ $Bebq_2$ and the UV-vis absorption/ PL spectra of RP411. As shown in Fig. 3, the wide overlap between the PL spectra of mCP/$Bebq_2$ and the UV-vis absorption spectra of RP411 makes it possible for the mCP/$Bebq_2$:RP411 to be a good host-dopant system for red phosphorescent emission. The chemical structures of mCP and $Bebq_2$ are shown in the inset of Fig. 3.

Current density-voltage and luminance-voltage characteristics of the fabricated devices are shown in Fig. 4 and Fig. 5, respectively. The shape of luminance-voltage curves is similar to the shape of current density-voltage curves because light of the OLEDs is induced by current injection. The highest values of current density and luminance at a given voltage were obtained in the device D with the HTIL of HATCN and the EIL of Cs_2CO_3. The current density and luminance of device D were 361 mA/cm^2 and 23,710 cd/m^2 under an

Table 1. Key electroluminescent characteristics of the fabricated devices

		Devices			
Parameters	Units	A	B	C	D
Driving Voltage (at 1000 cd/m^2)	V	6.3	5.2	4.9	3.3
Turn-on Voltage (at 1 cd/m^2)	V	3.9	3.1	2.9	2.0
Luminance (at 7 V)	cd/m^2	1820	6910	5910	23710
Current Density (at 7 V)	mA/cm^2	12	67	50	361
Efficiencies (at 1000 cd/m^2) Power	lm/W	7.6	8.5	8.6	13.4
Quantum	%	17.2	15.0	16.2	15.8
Peak Wavelength	nm	626	626	626	626
CIE	(x, y)	(0.67,0.32)	(0.67, 0.32)	(0.67,0.32)	(0.67,0.32)

applied voltage of 7 V, respectively. On the other hand, the current density and luminance of the other devices under the same voltage of 7 V were as follows: 12 mA/cm^2 and 1,820 cd/m^2 in the device A, 67 mA/cm^2 and 6,910 cd/m^2 in the device B, 50 mA/cm^2 and 5,910 cd/m^2 in the device C. The luminance of the device D was 13.0, 3.4, and 4.0 times higher than those of the device A, B, and C at an applied voltage of 7 V, respectively. This result shows that Cs_2CO_3 is more efficient than LiF as an EIL and the insertion of HATCN as an HTIL between HIL and HTL is very effective to increase current density and luminance of the OLEDs.

Power efficiency and quantun efficiency are very important parameters to evaluate the electro- luminescent characteristics of the OLEDs. The power and quantun efficiencies of the fabricated devices were shown in Fig. 6 and Fig. 7, respectively. The highest power efficiency at a given luminance was obtained in the device D as shown in Fig. 6. The power efficiencies of the fabricated devices at 1,000 cd/m^2 were 17.2% in the device A, 15.0% in the device B, 16.2% in the device C, and 15.8% in the device D. The quantum efficiency of the device D was somewhat lower than those of the device A and C, but a little higher than that of the device B as shown in Fig. 7. The power and quantun efficiencies showed the roll-off characteristics according to the increase of luminance. There have been several studies on the origin of efficiency roll-off in PhOLEDs [18,19]. Triplet-triplet annihilation was reported to be the main reason for the efficiency roll-off at high current density and it was dependent on the triplet exciton density. All of the quenching processes are closely related with the device structure. As the results of our experiments, the best electroluminescent characteristics could be obtained in the device D in terms of high power efficiency and high luminance without remarkable difference in the quantum efficiencies of the fabricated devices.

Electroluminescence (EL) spectra at an applied bias of 7 V were shown in Fig. 8. The peak wavelength of EL spectra was 626 nm for all of the fabricated devices. This means that most of light were generated from the triplets of RP411 with deep red emission of 1.98 eV. The color coordinates on the CIE chart were (0.67, 0.32) with color purity of more than 95%. The key electroluminescent characteristics of the fabricated devices were listed on Table 1.

4. Conclusion

The interfacial layers for hole transport and electron injection on the electroluminescent characteristics were investigated in the fabrication of red PhOLEDs. The HATCN was used as an interfacial layer for hole transport between HIL and HTL, and the LiF or Cs_2CO_3 as an EIL for electron injection in our experiments. The HATCN is a material with a deep LUMO level which can be well aligned to the HOMO levels of HIL and HTL. The Cs_2CO_3 is a material with the conduction energy level of 2.2 eV which can be well aligned to the Fermi level of metal, while the LiF is an insulator. The fabricated devices were divided into four kinds according to the adoption of HATCN between HIL and HTL and the choice of LiF or Cs_2CO_3 as an EIL.

At an applied voltage of 7 V, luminance of the devices with the Cs_2CO_3 as an EIL showed 3.8∼4.0 times as high as those of the devices with the LiF as an EIL, and luminance of the devices using the HATCN as an interfacial layer between DNTPD and TAPC showed 3.2∼3.4 times as high as those of the devices without the hole transport interfacial layer.. The luminance of the device D with the EIL of Cs_2CO_3 and the HTIL of HATCN showed 13.0 times as high as that of the device A without the HTIL using the EIL of LiF under a luminace of 1000 cd/m^2. The highest power efficiency under the same luminance was also

obtained in the device D even though the quantum efficiencies of the fabricated devices (A∼D) were similar in a range of 15.0∼ 17.2%.

The remarkable improvement of luminance and power efficiency in the device D comes from not only the efficient electron injection due to reduction of electron injection barrier in the EIL of Cs_2CO_3 as well as the hole transport enhancement by strong coulombic interaction with the aid of the HTIL of HATCN.

Acknowledgment

The present research was conducted by the research fund of Dankook University in 2014.

References

[1] Wetzelaer, G. A. H., Najafi, A., Kist, R. J. P., Kuik, M., & Blom, P. W. M. (2013). *Appl. Phys. Lett.*, *102*, 053301.
[2] Shangguan, R., Mu, G., Qiao, X., Wang, L., Cheah, K-W., Zhu, X., Chen, C-H. (2011). *Org. Electron.*, *12*, 1957.
[3] Chu, X. B., Guan, M., Niu, L. T., Zhang, Y., Li, Y. Y., Liu, X. F., & Zeng, Y. P. (2014). *Phys. Status Solidi. A.*, *7*, 1605.
[4] Chen, S., Jiang, X., So, F. (2013). *Org. Electron.*, *14*, 2518.
[5] Lee, C. W., Kim, O. Y., Lee, J. Y. (2014). *J. Ind. Eng. Chem.*, *20*, 1198.
[6] Hung, W-Y., Lin, C-Y., Cheng, T-L., Yang, S-W., Chaskar, A., Fan, G-L., Wong, K-T., Chao, T-C., Tseng, M-R. (2012). *Org. Electron.*, *13*, 2508.
[7] Kroger, M., Hamwi, S., Meyer, J., Riedl, T., Kowalsky, W., Kahn, A. (2009). *Org. Electron.*, *10*, 932.
[8] Mi, B. X., Gao, Z. Q., Cheah, K. W., & Chen, C. H. (2009). *Appl. Phys. Lett.*, *94*, 073507.
[9] Cai, Y., Wei, H. X., Li, J., Bao, Q. Y., Zhao, X., Lee, S. T., Li, Y. Q., & Tang, J. X. (2011). *Appl. Phys. Lett.*, *98*, 113304.
[10] Yang, J. S., Choo, D. C., Kim, T. W., Jin, Y. Y., Seo, J. H., Kim, Y. K. (2010). *Thin Solid Films*, *518*, 6149.
[11] Duan, L., Liu, Q., Li, Y., Gao, Y., Zhang, G., Zhang, D., Wang, L., & Qiu, Y. (2009). *J. Phys. Chem.*, *113*, 13386.
[12] Jeon, W. S., Park, J. S., Li, L., Lim, D. C., Son, Y. H., Suh, M. C., Kwon, J. H. (2012). *Org. Electron.*, *13*, 939.
[13] Diouf, B. B., Jeon, W. S., Park, J. S., Choi, J. W., Son, Y. H., Lim, D. C., Doh, Y. J., Kwon, J. H. (2011). *Synthetic. Met.*, *161*, 2087.
[14] Jeon, S. O., Yook, K. S., Joo, C. W., & Lee, J. Y. (2009). *Appl. Phys. Lett.*, *94*, 013301.
[15] Kim, T. Y., Moon, D. G. (2010). *Synthetic. Met*, *160*, 675.
[16] Park, Y. W., Jang, J. H., Kim, Y. M., Choi, J. H., Park, T. H., Choi, J., Ju, B. K. (2009). *Thin Solid Films*, *517*, 4108.
[17] Ji, H. J., & Jang, J. G. (2013). *Mol. Cryst. Liq. Cryst.*, *584*, 78.
[18] Wang, Z. B., Helander, M. G., Qiu, J., Puzzo, D. P., Greiner, M. T., Liu, Z. W., & Lu, Z. H. (2011). *Appl. Phys. Lett.*, *98*, 073310.
[19] Jeon, S. O., Yook, K. S., Joo, C. W., Lee, J. Y. (2010). *Org. Electron.*, *11*, 881.